Surface acid-base properties of anion adsorbed species at Pt(111) electrode surfaces in contact with CO_2 containing perchloric acid solutions.

R. Martínez-Hincapié, A. Berná, A. Rodes, V. Climent, J.M. Feliu*.

Instituto de Electroquímica y Departamento de Química Física. Universidad de Alicante. 03080 Alicante. Spain

Abstract:

Carbonate and bicarbonate adsorption on Pt(111) electrodes from CO_2 saturated acidic solutions is investigated by cyclic voltammetry and Fourier Transform Infrared Reflection Absorption Spectroscopy (FT-IRRAS). Spectroscopic results show carbonate and bicarbonate adsorption even at pH=1, where bulk concentration of these anions is negligible. Moreover, analysis of the potential dependence of band intensities corresponding to adsorbed carbonate and bicarbonate reveals an effect of the electrode potential on the surface acid-base equilibrium. In this regards, increasing potentials favor bicarbonate deprotonation, leading to carbonate formation. A tentative thermodynamic analysis is given to rationalize these trends.

1. Introduction.

The understanding of interfacial properties is a challenging topic in physical electrochemistry and requires careful experiments combining different techniques. One of the classical subjects in this field deals with the specific adsorption of anions. This topic has already been addressed on mercury electrodes[1] and extended later to coinage[2-4] and platinum group metal electrodes[5-8] to explore the validity of double layer models. These investigations have important implications in practical electrochemistry, since anion adsorption competes with other molecular species, either reagents or intermediates, in electrocatalytic reactions, thus hindering the reaction rate. As an example, oxygen reduction shifts to lower potentials in

sulphuric acid as compared with perchloric acid solutions[9] because sulphate adsorption influences relevant steps in the activation mechanism. Moreover, if the anion adsorption strength is high enough, the 4e reduction process to water will stop at the peroxide stage (2e).[10] In this case, anion adsorption not only affects the mechanism but also the stoichiometry of the overall reaction.

The fact that anion adsorption at platinum electrodes involves charge transfer was shown many years ago by using the CO-displacement methodology.[11-13] This experiment was used to clarify the nature of the adsorption processes which are at the origin of the voltammetric profiles recorded for platinum single crystal electrodes. The obtained results helped in the understanding of the coulometric relationships related to the stoichiometry of surface confined reactions.[14] Moreover, important interfacial parameters, such as the potentials of zero charge of platinum-group metals, were defined in connection with these experiments and anion adsorption was shown to take place at potentials higher than the potential of zero total charge.[7, 15] Thermodynamic analysis allowed the determination of parameters associated to this process, such as charge transfer numbers and energies of adsorption.[6, 8, 16-18] When the study includes a surface acid base equilibrium, pH variation allows discrimination of the nature of the adsorbed species. [4, 19] In this way, it was demonstrated that Pt(111) in contact with sulphuric acid solutions led to sulphate adsorption,[19] in agreement with results from other experimental techniques.[20]

These studies demonstrate that composition of the interphase can often be significantly different from that of the bulk of the solution. For instance, sulfate is adsorbed on the Pt(111) surface from sulfuric acid solutions, while the predominant species in the bulk is bisulfate.[19] A similar situation has been observed with anions ((bi)oxalate, (bi)malonate and (bi)succinate) coming from several dicarboxylic acids. In general, a lower pK_a is observed for the adsorbed species as compared with the pK_a of the species in solution.[21-22] By comparing dicarboxylic

acids with different lengths of the alkyl chain, it was demonstrated that the effect of the electric field on the pK_a of the uncoordinated carboxylate decreases as its separation from the electrode surface increases. [21-22] Another interesting example is the adsorption of carbonate and bicarbonate from perchloric acid solutions saturated with CO_2.[23-26] Taking into account the corresponding pK_a values, the concentration of anions in the bulk should be negligible in acidic solutions (e.g. around 10^{-7} and 10^{-17} M, respectively, for bicarbonate and carbonate in solutions of pH 1) and thus unable to generate the measured voltammetric adsorption charges.[27] However, the analysis of in situ Fourier Transform InfraRed Reflection Absorption (FT-IRRAS) spectra, based on Density Functional Theory (DFT) calculations for band assignment, pointed out that the adsorbed layer was formed by bicarbonate and carbonate anions, with bicarbonate being adsorbed at lower potentials, while carbonate bands appeared at higher potentials. [25] This trend was pH-dependent, in such a way that the onset of carbonate adsorption moved to lower potentials as the pH is made less acidic.[25]

From the latter results, it can be assumed that adsorbed bicarbonate and carbonate anions are present on the electrode surface in the acidic CO_2-containing solutions. From the analysis of the pH- and potential-dependence of the corresponding band intensities, which can be related to changes in the carbonate and bicarbonate surface coverages, the conditions (pH and potential) to reach equal population of both adsorbed species can be found and used to estimate the surface pKa value. In this paper, we investigate the surface equilibrium between adsorbed carbonate and bicarbonate at Pt(111) electrodes in contact with acidic solutions of a non-specifically adsorbing supporting electrolyte. The effect of pH and potential on this equilibrium is analyzed in connection to the corresponding concepts of surface charge density and, thus, the electric field at the electrode surface.

2. Experimental.

Platinum single crystal electrodes were oriented, cut and polished from single crystal beads as reported previously.[28] Before each experiment, the electrode was flame annealed in a Bunsen flame, cooled down in a reducing atmosphere containing H_2 + Ar and protected with water in equilibrium with this gas mixture to prevent contamination and the appearance of surface defects related to oxygen adsorption. The voltammetric experiments were carried out in a classical three electrode configuration, at room temperature. Working solutions were first deaerated by Argon bubbling and, after checking solution cleanliness by voltammetry, saturated with CO_2. The counter electrode was a large coiled platinum wire, while a reversible hydrogen electrode (RHE) was used as reference, connected to the cell through a Luggin capillary. Potentials were converted to the SHE scale and are given in this scale throughout the paper. The measurements were performed with a EG&G PARC 175 signal generator, an eDAQ EA161 potentiostat and an eDAQ e-corder ED401 recording system. The pH of the solution was determined with a Crison 507 pH-meter.

In situ external reflection infrared experiments were carried out with a Nicolet 8700 (Thermo Scientific) spectrometer equipped with a MCT-A detector using p-polarized light and with a spectral resolution of 8 cm^{-1}. The glass spectroelectrochemical cell was equipped with a prismatic CaF_2 window bevelled at 60°, a platinum counter electrode and a RHE reference electrode. The Pt(111) working electrode used in these experiments was ca. 4.5 mm in diameter and was prepared and treated before experiments in a similar way as the smaller samples used in the voltammetric experiments. The spectra are plotted in absorbance units ($-\log(R/R_0)$) by referring the single beam reflectance spectrum collected at the sample potential (R) to that collected at the reference potential (R_0), which was chosen at 0.10 V. As the adsorption / desorption processes studied in this work are reversible with respect to the electrode potential, the so-called SNIFTIR (substractively normalised FTIR [29]) is used. Thus, 10

sets of 100 interferograms were collected alternately at the sample and reference potentials. Positive- and negative-going bands in the spectra correspond, respectively, to species being formed/consumed when collecting the sample single beam spectrum.

3. Results and discussion.

3.1.Voltammetric and Spectroscopic results

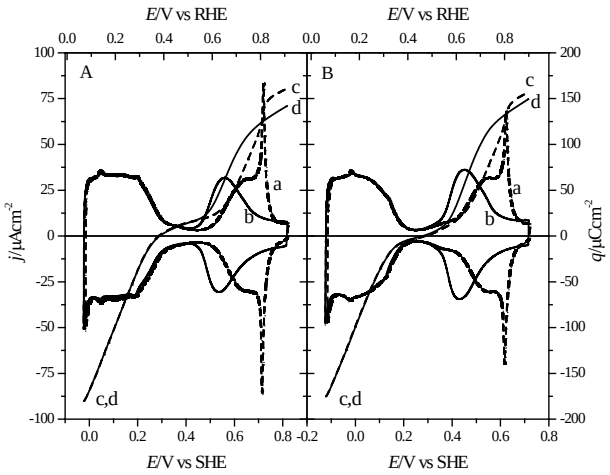

Figure 1. Cyclic Voltammograms (a,b, left-hand axis) and total charge density (c,d, right-hand axis) for Pt(111) in (0.1-x) M $KClO_4$ + x M $HClO_4$ solutions with (solid line) and without (dashed line) CO_2 . A) pH 1.56 and B)pH 3.10.

Curves a and b in Figures 1A and B shows the voltammetric profiles of Pt(111) electrodes in contact with perchloric acid solutions of different pH in absence and presence of saturated CO_2 gas. The rather flat current profile at E<0.30 V indicates the nearly absence of defects on this surface.[30-32] The negative shift of the typical voltammetric features for the Pt(111) electrode at potentials between 0.50 and 0.90 V in the CO_2-containing solutions can be related to reversible specific adsorption of anion species. The total charge/potential plots (curves c and d) were obtained from the integration of the voltammetric curves by using the charge displaced by CO at 0.1 V to define the constant of integration.[7, 15, 33] Displaced charges by CO were corrected to

account for the remaining charge on the CO saturated surface.[34-35] The positive values of charge at potentials above ca. 0.50 V indicate the adsorption of anion-like species, namely carbonate and/or bicarbonate in the CO_2-containing solutions, as described previously. [23-25] Regarding adsorption/desorption processes at low potentials, it can be remarked that both voltammetric and charged density curves in the hydrogen adsorption regions are coincident, with and without CO_2, signaling that anion adsorption does not imply charge transfer in this potential region. Similarly, potentials of zero total charge (pztc) [7, 15, 33] are nearly the same in the presence or absence of CO_2 in solution. Table 1 summarizes, for two solution pH values, the values of the pztc and the potential of zero free charge (pzfc) (as extrapolated from the double layer region. [36-37]) The same can be said for the corresponding values after correction for the residual charge of the CO-covered surface.[34-35] Currents and charges in the presence and absence of CO_2 coincide also for most of the double layer region, while the onset of (bi)carbonate adsorption is negatively shifted in comparison with the onset of OH adsorption in pure perchlorate/perchloric acid solutions.

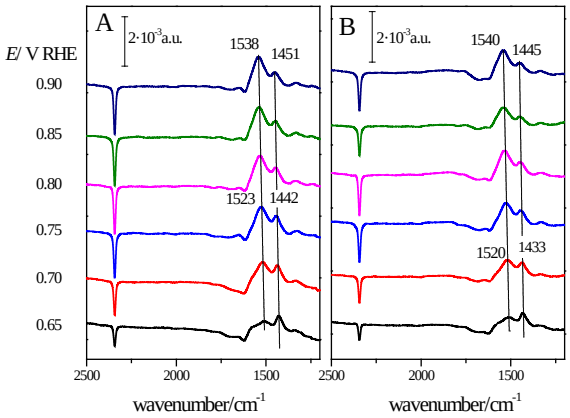

Figure 2. FTIRRAS spectra for Pt(111) obtained with p-polarized radiation at various sample potentials in solutions saturated with CO_2 A) pH 1.56 and B) 2.47. The reference spectrum was collected at 0.1 V. (10x100) interferograms were collected at each potential.

Figures 2A and B show sets of external reflection infrared experiments collected for the Pt(111) electrode in contact with CO_2-saturated perchloric acid solutions with pH equal to 1.56

and 2.47, respectively. One of the main features in these spectra is a negative-going band appearing at 2344 cm^{-1} that can be assigned to the asymmetric O-C-O stretching mode of dissolved carbon dioxide molecules whose concentration in the thin layer solution decreases when stepping the electrode from 0.10 V to the sample potential. This consumption is detected for potentials above 0.60 V and increases when the electrode potential value is made more positive (i.e. in the potential region where characteristic broad voltammetric features are observed in the CO_2-containing solutions (see Figures 1A and B)). The raise of the CO_2 band intensity is paralleled by the development of positive-going features at ca. 1530, 1440 and 1330 cm^{-1} that can be assigned to adsorbates formed from the CO_2 molecules. This latter conclusion is based both on the potential-dependent band frequency and their absence in the spectra collected with s-polarized light.[24-25] DFT calculations showed that the band at ca. 1530 cm^{-1} can be assigned to the C-O stretching of the uncoordinated CO bond of carbonate anions adsorbed in short bridge sites,[25] whereas the feature at ca. 1440 cm^{-1} can be related to bicarbonate anions adsorbed also in short bridge sites. The small band at 1330 cm^{-1} in water solutions, which is not observed in the spectra collected in deuterium oxide solution, was also assigned to adsorbed bicarbonate anions (namely, to the C-OH bending mode that would be shifted to lower wavenumbers in the case of the C-OD bending).[25] All these assignments suggest the presence of coadsorbed carbonate and bicarbonate anions for potentials above 0.60 V. This conclusion is consistent with the observation of a relative increase of the bicarbonate bands in the spectra collected, at a given electrode potential, in more acidic solution (see Figure 3). Thus, it can be suggested the existence of a surface equilibrium between coadsorbed carbonate and bicarbonate species that can only be observed for the corresponding dissolved species in more alkaline solution. In other words, the equilibrium constant between adsorbed carbonate and bicarbonate anions seems to be much higher than in the case of dissolved species. Besides, changes in the relative intensities of the adsorbed

carbonate and bicarbonate features when changing the electrode potential suggests the existence of an effect of the latter on the value of the surface equilibrium constant.

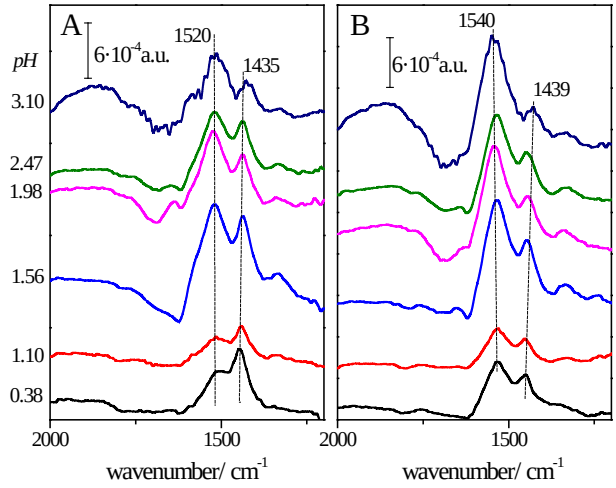

Figure 3. In situ FTIRRAS spectra for Pt(111) obtained with p-polarized radiation at different pHs in solutions saturated with CO_2 A)0.70 V and B) 0.80 V vs RHE. The reference spectrum was collected at 0.1 V. (10x100) interferograms were collected at each potential.

3.2 Quantitative analysis of band intensities

Figure 4A and C reports data corresponding to the integrated intensities of carbonate and bicarbonate bands for pHs equal to 0.38 and 1.56. Since these bands are partially overlapped, to obtain the integrated intensities of each separate band it is necessary to decompose them by adjusting to Lorentzian functions.[38] These plots allow the comparison of deconvoluted intensities of carbonate and bicarbonate with the integrated intensity of the CO_2, as a function of the electrode potential. Trends in the integrated intensities are the same as those already discussed when comparing the in situ spectra in Figure 2. The CO_2 band intensity increases (negatively) with the electrode potential from 0.65 to 0.75 V and then reaches a nearly constant plateau between 0.75 to 0.90 V. Carbonate and bicarbonate band intensities also increase (positively) in the potential region where CO_2 band intensity is increasing, demonstrating that the CO_2 depletion is linked with carbonate/bicarbonate adsorption. At potentials above 0.75 V, bicarbonate band intensity decreases while carbonate band intensity

increases. This happens in the region where CO_2 intensity is nearly constant, i.e., without further increase of total coverage of (bi)carbonate adsorbed species. Therefore, the intensity variation above 0.75 V indicates a conversion of bicarbonate into carbonate triggered by the increase of the electrode potential, indicating that there is an effect of the latter on the acid-base surface equilibrium.

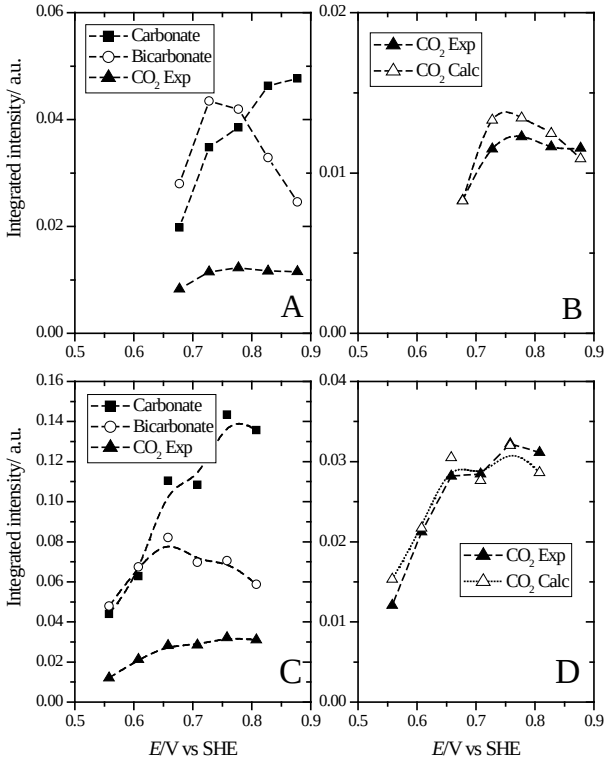

Figure 4. A and C) Integrated intensity for CO_2 and adsorbed carbonate and bicarbonate bands on Pt(111) at pH 0.38 (A) and 1.56 (C); B and D) Comparison of experimental CO_2 band intensities (full symbols) and calculated from carbonate and bicarbonate band intensities (empty symbols) at pH 0.38 (B) and 1.56 (D). (See text for details)

To perform a further quantitative analysis of the in situ infrared spectra, with the aim of determining surface or solution concentrations from band intensities, it should be accepted that the absorption bands obey Lambert-Beer law. If this is so, integrated intensities of the absorption bands, in absorbance units, are directly proportional to the concentration of the chemical species generating this particular vibrational mode. The proportionality constant includes two terms: the optical length distance, *l*, and the molar absorption coefficient or

molar absorptivity, ε^{j}_{i}, of the band with frequency *j* corresponding to the species *i*. The corresponding expression of the integrated absorbance for the band of a non-adsorbed species, such as dissolved CO_2, would have the form:

$$A_{CO_2(disol.)} = \varepsilon^{2343}_{CO_2} \cdot l \cdot C_{CO_2(disol.)} \quad (1)$$

For adsorbed carbonate and bicarbonate, the analogous expressions would be:

$$A_{HCO_3(ads.)} = \varepsilon'^{1440}_{HCO_3} \cdot \Gamma_{HCO_3(ads.)} \quad (2)$$

$$A_{CO_3(ads.)} = \varepsilon'^{1530}_{CO_3} \cdot \Gamma_{CO_3(ads.)} \quad (3)$$

Where $\varepsilon'^{j}_{i} = \varepsilon^{j}_{i} \cdot l$.

The determination of the exact values of the molar absorption coefficients of adsorbed species is not an easy task, because the mean electromagnetic field of the radiation on the surface depends on multiple parameters such as the thickness of the thin layer between the prism and the metal electrode, the angle of incidence, and the optical properties of the surface [29] Moreover, the molar absorptivity for adsorbed species would include any electronic effect caused by the bonding to the metal surface, which can be expected to be potential-dependent.[39] Also, the eventual effect of the electrode potential on the orientation of the dynamic dipole moment with respect to the normal to the surface would affect the value of ε'^{j}_{i} .[39-40] For all these reasons, it has to be assumed that the absorption molar coefficients in equations (1-3) can be different from those that would be obtained in solution.

Thus, the determination of absolute surface concentration of adsorbed species from the spectroscopic data reported above involves knowledge of parameters usually non available. However, the ratio of surface coverages for two adsorbed species (such as carbonate and bicarbonate anions) can be calculated by performing a material balance within the thin layer in which the external reflection spectroelectrochemical experiments are carried out:

$$\Delta n_{CO_2(sol.)} = n_{HCO_3(ads.)} + n_{CO_3(ads.)} \quad (4)$$

In this equation *n* for carbonate and bicarbonate refer to the corresponding number of adsorbed moles of each species at a given electrode potential and solution pH values whereas Δ*n* for carbon dioxide stands for the number of moles in the thin layer being consumed upon carbonate and/or bicarbonate adsorption. Note that, as a difference with ATR-SEIRAS experiments [41-42] this balance can be analyzed from the external reflection experiments due to the decoupling of mass transport between the thin layer sampled by the infrared beam and the bulk working solution. In this material balance, we have to assume that, due to the short time elapsed in the SNIFTIR experiment during the collection of the reference and sample single beam spectra (43 s for 100 interferograms), there is not extra increase of CO_2 molecules in the thin layer coming from the bulk. A non-negligible replenishment of the CO_2 molecules consumed upon carbonate and bicarbonate adsorption would lead to a value of the integrated intensity for CO_2 slightly lower that the correct one.

Equation (4) can be rewritten as function of the corresponding surface and volume concentrations:

$$V_{tl} \cdot C_{CO_2(sol.)} = S \cdot \Gamma_{HCO_3(ads.)} + S \cdot \Gamma_{CO_3(ads.)} \quad (5)$$

Where *S* is the area of the electrode and V_{tl} is the volume of the thin layer, that can be written as

$$V_{tl} = S \cdot d_{tl} \quad (6)$$

where d_{tl} is the thickness of the thin layer. All other symbols in equation (5) have their usual meaning. After substituting equations ((1)-(3) and (6) in equation(4)) we reach the following expression:

$$d_{tl} \cdot \frac{A_{CO_2}}{\varepsilon_{CO_2}^{2343} \cdot l_{CO2}} = \frac{A_{HCO_3(ads.)}}{\varepsilon_{HCO_3}^{'1440}} + \frac{A_{CO_3(ads.)}}{\varepsilon_{CO_3}^{'1530}} \quad (7)$$

After reordering, we get:

$$A_{CO_2} = K_1 \cdot A_{HCO_3(ads.)} + K_2 \cdot A_{CO_3(ads.)} \quad (8)$$

Where

$$K_1 = \frac{\varepsilon^{2343}_{CO_2} \cdot l_{CO2}}{\varepsilon^{'1440}_{HCO_3} \cdot d_{tl}} \quad (9)$$

$$K_2 = \frac{\varepsilon^{2343}_{CO_2} \cdot l_{CO2}}{\varepsilon^{'1530}_{CO_3} \cdot d_{tl}} \quad (10)$$

If we accept that the ratio between molar absorption coefficients is constant and independent of the electrode potential (that is, the bonding with the surface affects in the same way molar absorption coefficients for both adsorbed carbonate and bicarbonate and there is no potential-dependent reorientation of these adsorbates) it would be possible to relate the experimental integrated intensity data of the CO_2 band with those of the adsorbed carbonate and bicarbonate. The K_1 and K_2 terms in equation (8) depend of the particular experimental conditions, such as the optical length, l_{CO2}, and the thin layer thickness, d_{tl}. For this reason, they will be different for each experiment. However, the ratio between them should be constant, because in fact, they correspond to the ratio between the molar absorption coefficients of the adsorbed carbonate and bicarbonate anions:

$$\frac{K_1}{K_2} = \frac{\dfrac{\varepsilon^{2343}_{CO_2} \cdot l_{CO2}}{\varepsilon^{'1440}_{HCO_3} \cdot d_{tl}}}{\dfrac{\varepsilon^{2343}_{CO_2} \cdot l_{CO2}}{\varepsilon^{'1530}_{CO_3} \cdot d_{tl.}}} = \frac{\varepsilon^{'1530}_{CO_3}}{\varepsilon^{'1440}_{HCO_3}} \quad (11)$$

By combining this ratio between the molar absorption coefficients with that between bicarbonate and carbonate surface concentrations derived from equations (2) and (3) we obtain:

$$\frac{\Gamma_{HCO_3(ads.)}}{\Gamma_{CO_3(ads.)}} = \frac{\varepsilon'^{1530}_{CO_3}}{\varepsilon'^{1440}_{HCO_3}} \cdot \frac{A_{HCO_3(ads.)}}{A_{CO_3(ads.)}} = \frac{K_1}{K_2} \cdot \frac{A_{HCO_3(ads.)}}{A_{CO_3(ads.)}} \quad (12)$$

K_1 and K_2 values can be estimated by comparing experimental values for the integrated intensities for the carbon dioxide consumption band with values calculated from equation (8) using experimental values for the integrated intensities of adsorbed carbonate and bicarbonate bands. This was done by a least square fitting of equation (8) to experimental band intensities for all the data sets at different pHs (from 0.38 to 3.0) using Solver routine of Microsoft Excel. The obtained values for K_1 and K_2 are, respectively, 0.245 and 0.136. Comparison with the experimental values of the calculated CO_2 integrated intensities using these values of K_1 and K_2 and equation (8), are presented in figures 4C and D. These plots show a quite good agreement between experimental and calculated values, except at high potentials, likely due to the competition of other possible adsorbates, such as PtOH. Note that the ratio between the molar absorption coefficients of carbonate and bicarbonate obtained from K_1 and K_2, 1.78, is quite close to that found in solution for the characteristic bands of dissolved carbonate and bicarbonate, which is 2. [43] Thus, it can be concluded that, as assumed in the case of anions from dicarboxylic acids,[21-22] adsorption does not affect the ratio of molar extinction coefficients (in this case, of carbonate and bicarbonate anions) in a significant way.

3.3. Thermodynamic considerations

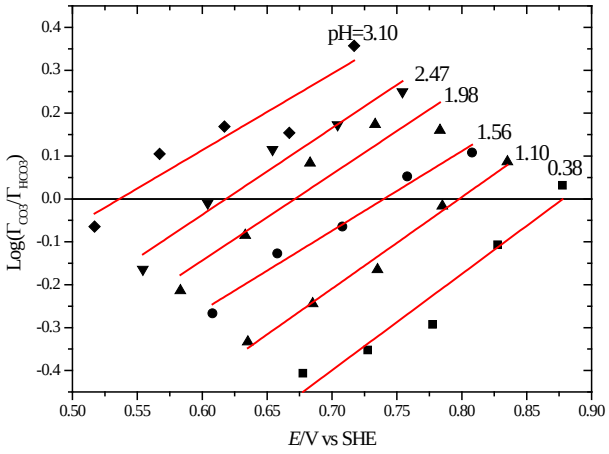

Figure 5. Ratio of surface concentrations for carbonate and bicarbonate as a function of electrode potential in solutions with different pHs, as labelled in the figure.

Calculated ratios for bicarbonate and carbonate coverages obtained from the latter analysis of band intensities are plotted in Figure 5 as a function of the electrode potential for the studied solution pHs. As already anticipated above, there is a clear effect of the electrode potential on the acid base equilibrium, with the increase of the potential favoring the deprotonation of the bicarbonate and the formation of adsorbed carbonate. This can be rationalized qualitatively by invoking different arguments. First we could consider the effect of electron density withdrawing associated with an increase of electrode potential that will increase the acidity of the OH group of the adsorbed bicarbonate. This would be similar to the induction effect well known to affect the acidity of organic acids depending on the electronegativity of the substituents next to the carboxylate group.[44]

On the other hand, a direct effect of increasing values of the electric field at the metal / solution interphase could also be considered. The effect of high electromagnetic fields on certain chemical properties has been extensively analyzed in the literature, but especially significant to this work is the effect over the equivalent electric conductivity of electrolytes. This aspect was thoroughly studied by M. Wien in his work from 1920's.[45-48] Wien found that under high electromagnetic fields, electrolytes start to disobey ohm's law and the conductance

of electrolytic solutions increases with the intensity of the applied electromagnetic field. In a first stage, only strong electrolytes were studied and this effect, called the first or normal Wien effect,[45-47] was determined as an inherent property of electrolytic solutions, depending on the concentration and charge of the ions and the specific character of the solute and the solvent. When these studies were extended to weak electrolytes, the effect of high electromagnetic fields on the electric conductance of the solutions turned out to be many times larger than in the case of strong electrolytes. In this case, the explanation to this effect has to be attributed to another phenomenon different to the first Wien effect. Wien suggested that in the case of weak electrolytes, the increase in the electric conductivity of these solutions was due to an increase in the acid dissociation constant.[48] This explanation was confirmed by the work of L. Onsager,[49] who establish an equation for the relationship between the change in the acid dissociation constant and electromagnetic field. This effect is called the second Wien effect or the dissociation field effect.[48-49] The electromagnetic field weakens the acid hydrogen and the conjugated base increasing the kinetic constant for the dissociation reaction but not altering the kinetic constant for the recombination reaction.[49] This phenomenon has a net effect of increasing the acid-base equilibrium constant and therefore the dissociation degree. This phenomenon has been determined for the evaluation of acid-base equilibrium constants in weak acids in the electrochemical double layer region using rotating disk electrodes by Vielstich.[50] In Vielstich work, the effect was evaluated for weak acids in solution and changes in the acid-base equilibrium constant of more than one order of magnitude were observed. In the case of adsorbed weak acids, the electromagnetic field intensity could be even higher and, therefore, deep changes in the acid-base equilibrium constant have to be expected.

The effect of electrode potential on the acid-base equilibrium can be further analysed on a thermodynamic basis by considering the following surface reaction:

$$HCO_3^{x-}(ads) \quad CO_3^{y-}(ads) + H^+ + (1 + x - y)e \qquad (13)$$

Where (*x*-*y*) will be called *z* in the following and would represent the difference between the formal surface oxidation numbers of bicarbonate and carbonate, respectively. If both anions are totally discharged upon adsorption, *x*=*y*=0 and the acid base equilibrium involves also the transfer of one electron. On the other hand, if *x*=0 but *y*=1, i.e., the adsorbed carbonate is not totally discharged, the surface equilibrium would be purely a proton release without charge transfer. The same situation would also happen if *x*=1 and *y*=2, namely, if both anion adsorptions do not involve charge transfer, although this situation is less likely as suggested by CO displacement experiments. The (electro)chemical equilibrium condition for this reaction can written in terms of (electro)chemical potentials:

$$\sum \nu_i \bar{\mu}_i = 0 \tag{14}$$

This condition can be applied in this case since equilibrium is attained at each potential as deduced from the symmetry of the cyclic voltammogram. Electrochemical potentials of adsorbed species are given by[51-52]:

$$\bar{\mu}_{i_{ads}} = \mu^0_{i_{ads}} + RT \ln \frac{\Gamma_i}{\Gamma_{m,i} - \Gamma_i} + z_i F \Phi_i \tag{15}$$

with $\Gamma_{m,i}$ being the maximum surface concentration of species *i*. Here we have considered Langmuirian behaviour for adsorbed species and therefore neglected additional terms such as those derived from the existence of lateral interactions. For species in solution

$$\bar{\mu}_i = \mu^0_i + RT \ln(a_i) + z_i F \Phi_s \tag{16}$$

In these equations, Φ_i is the electric potential at the location where the reaction is taking place and Φ_s is the electric potential at the bulk of the solution. These equations lead to the following Nernst equation:

$$E = \frac{\Delta G^0}{(1+z)F} + \frac{RT}{(1+z)F} \ln \frac{a_{H^+,s} \Gamma_{CO_3}}{\Gamma_{HCO3}} + (\Phi_i - \Phi_s) \frac{z}{1+z} \tag{17}$$

Where

$$\Delta G^0 = \mu^0_{CO_3} + \mu^0_{H^+} - \mu^0_{HCO_3} - (1+z)\sum_{ref}\mu^0_i \tag{18}$$

$\sum_{ref}\mu^0_i$ is a combination of standard chemical potential of species involved in the reference electrode. Moreover, the proton activity at the plane of adsorbed species $a_{H^+,i}$ and the activity at the bulk of the solution $a_{H^+,s}$ are related by:

$$\Phi_i - \Phi_s = -\frac{RT}{F}\ln\frac{a_{H^+,i}}{a_{H^+,s}} \tag{19}$$

This equation, derived from the equality of electrochemical potentials $\overline{\mu}_{H^+,i} = \overline{\mu}_{H^+,s}$,is equivalent to the Boltzmann distribution of ions in the electric field near the electrode surface.

In the particular case where *z*=-1 equation (17) reduces to:

$$RT\ln\frac{a_{H^+,s}\Gamma_{CO_3}}{\Gamma_{HCO3}} = -\Delta G^0 + F(\Phi_i - \Phi_s) \tag{20}$$

Except for the term $F(\Phi_i - \Phi_s)$ this is the traditional definition of the equilibrium constant for the acid-base reaction. The term $F(\Phi_i - \Phi_s)$ has to be included to account for the different concentration of protons induced by the electric field. If we neglect, as a first approximation, the difference between the electric potential at the plane of adsorbed species and the bulk solution, after some reordering, equation (17) becomes

$$\log\frac{\Gamma_{CO_3}}{\Gamma_{HCO_3}} = \frac{(1+z)F}{RT\ln(10)}(E - E^0) + pH \tag{21}$$

According to this equation, the plot of figure 5 should be linear with a slope (1+*z*)/0.059 V^{-1}= 16.9 (1+z) V^{-1}. The experimental slope of the plots of figure 5 are around (2.1 ± 0.2) V^{-1},

resulting a value of *z* of ca: -0.88. If we assume that bicarbonate is totally discharged upon adsorption, x=0, and y=-0.88. Similar values of charge transfer numbers are obtained for adsorbed sulfate, [8, 53] indicating that these anions are not completely discharged in the adsorbed state. The low slope values mentioned above indicate that the description of the deprotonation in equation (13) as whole electron transfer process might not be accurate and the process would be better described as just a partial reorganization of charges at the interphase as a consequence of the deprotonation. In other words, while there is a shift of the acid base equilibrium with the potential, this effect is much lower than that expected from a whole electron transfer following Nernst law.

An alternative description would involve equation (20), i.e., a plain acid-base equilibrium, with the term $(\Phi_i - \Phi_s)$ resulting from the different concentration of protons at the surface in comparison with the bulk. The latter term would be the one accounting for the potential dependence of the equilibrium constant. According to equation (20) the plot of $\log \Gamma_{CO_3} / \Gamma_{HCO3}$ as a function of pH would give a straight line with slope of 1 if the term $(\Phi_i - \Phi_s)$ is constant. This term would depend on the free charge on the interphase, on the anion coverage and on its formal surface oxidation number. We attempted such plots at constant potential, *E*, and at constant total and free charges (not shown). In all cases, slopes significantly lower than unity were obtained, suggesting that equation (20) does not give a complete description of the phenomena either, and some partial charge transfer or charge reorganization has to be taken into account to explain the potential dependence.

The effect of the term $(\Phi_i - \Phi_s)$ on the rate of reaction rates was introduced by Frumkin and therefore is sometimes called the Frumkin effect.[54] This term account for two effects: i) the effective potential difference at the plane of the reacting species is different from the whole potential drop measured from the metal to the bulk of the solution and ii) the concentration of ionic species at the plane of the reaction is different from the concentration at the bulk

according to Boltzmann distribution. In the context of the present study, this term should be introduced to account for the difference between the surface and bulk pH. In the absence of specific adsorption this term is usually estimated using Gouy-Chapman theory. Although this theory would not be applicable in the present case, due to the adsorption of (bi)carbonate, we give in table 2 some values resulting from the application of this model, considering Φ_2 (at the OHP) as an estimation of Φ_i , just to get an indication of the magnitude of this term. We observe that surface pH can be significantly more alkaline than the bulk pH as a consequence of the introduction of positive charges at the interphase.

In addition to the pure electrostatic effect just discussed, there are other reasons that could affect the value of the interfacial pH. As discussed above, the electromagnetic field at the interphase can affect the acidity of water, the same as it affects the acidity of weak acids. Also, the specific interaction of water with the metal surface could affect the autoprotolysis equilibrium. Finally, it has been recently reported that acidity of water surfaces is significantly different (more acidic) than bulk water.[55] The reason for this is that H_3O^+ ions exhibit enhanced stability at the surface while OH^- does not. Bulk water can form two proton donor bonds and two proton acceptor bonds, resulting in tetrahedral networks. Because H_3O^+ ions can only form three protons – donor bonds but has poor capacity to form a proton acceptor bond, H_3O^+ ions have a disrupting effect on the tetrahedral network and can be better accommodated on the surface. To include such effect in the thermodynamic treatment above, equation (19) need to be transformed into:

$$\left(\Phi_i - \Phi_s\right) + \frac{\left(\mu^0_{H^+,i} - \mu^0_{H^+,s}\right)}{F} = -\frac{RT}{F}\ln\frac{a_{H^+,i}}{a_{H^+,s}} \qquad (22)$$

where the difference in standard chemical potentials accounts for the different chemical environment of H^+ at the interphase and in the bulk of the solution. In this regard, coulometric measurement on the Pt(111) surface in contact with perchlorate / perchloric acid mixtures of

different pH led to the conclusion that the neutral condition at the interphase is achieved for a value of pH at the bulk significantly lower than 7 (around 3.5), indicating that the equilibrium of the autoprotolysis of water is significantly affected by the particular environment present at the interphase.[36-37]

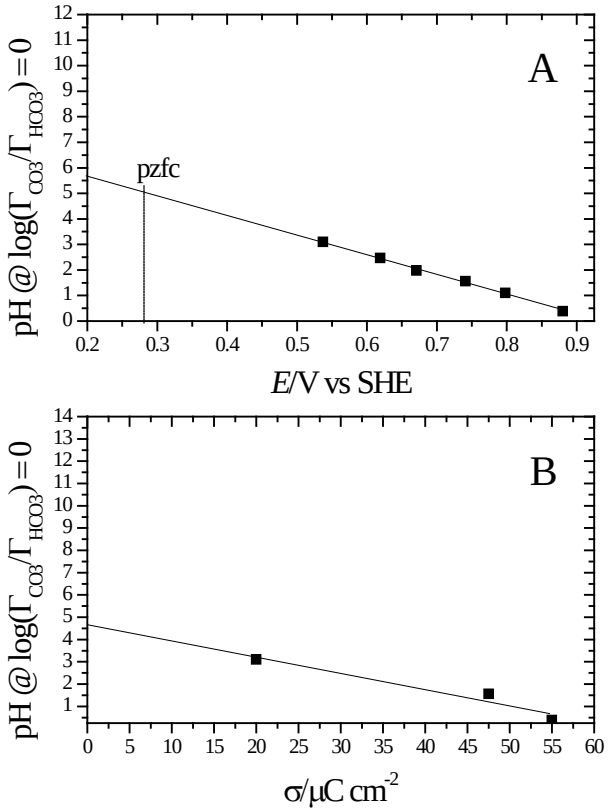

Figure 6. Value of pH where log($\Gamma_{CO3}/\Gamma_{HCO3}$)=0 as a function of potential (A) and free charge value (B), as obtained from the plots in Fig. 5 (see text for details).

In Figure 5 the lines cross zero when both surface concentrations are equal. For a pure acid base equilibrium this point would define the value of the pK_a of the adsorbed acid at each potential. The resulting values are plotted in figure 6. Figure 6A plots the results as a function of potential, while figure 6B shows the same plot using the free charge as independent variable. Free charge values were extrapolated from the double layer region assuming constant value of double layer capacity. In both cases the plot is linear. An interesting point

would be the value of the pH for equal surface excesses, when the free charge at the interphase is cero. According to the plot in Fig 6B, this is achieved at a value of pH around 4.5 $\pm$ 0.5. Similar result is obtained from the plot of Fig 6A, considering that pzfc is ca 0.28 V SHE. For a pure acid-base equilibrium in the bulk of the solution this would represent the pK_a of the acid under scope, which for bicarbonate is 10.3. In conclusion, the effect of adsorption is a significant decrease of the acidity constant for bicarbonate adsorbed on Pt(111), even if the obtention of exact values for surface pK_a is limited by the uncertainties discussed above.

4. Conclusions

A voltammetric and spectroscopic study of carbonate and bicarbonate adsorption on Pt(111) has revealed that these species adsorb on the electrode surface even from solutions with acidic pH, where the corresponding bulk concentrations are negligible. This result points towards a significant different value of the pK_a for bulk and adsorbed species. Careful analysis of band intensities shows an interconversion between adsorbed carbonate and bicarbonate, with high potentials favouring deprotonation of bicarbonate. One important conclusion is that the acidity of adsorbed bicarbonate is much higher than that of the anion in the bulk solution and the difference increases with the increase of the potential. Inductive effect of the positive polarization on the acidity of the adsorbed carboxylate or a direct effect of the electric field on the dissociation constant (similar to the second Wien effect) can be claimed to qualitatively rationalise the observed trends. A tentative thermodynamic treatment is presented, quantitative results being probably affected by the effect of electrode potential on the local pH at the surface of the electrode.

Acknowledgements

Support from MINECO (Spain) through project CTQ2013-44083-P is greatly acknowledged. RMH thankfully acknowledges support from Generalitat Valenciana under the Santiago Grisolia Program (GRISOLIA/2013/008).

References

1. Grahame, D. C., The electrical double layer and the theory of electrocapillarity. *Chem. Rev.* **1947**, *41*, 441-501.
2. Lipkowski, J.; Shi, Z. C.; Chen, A. C.; Pettinger, B.; Bilger, C., Ionic adsorption at the Au(111) electrode. *Electrochim. Acta* **1998**, *43*, 2875-2888.
3. Hamelin, A., Double layer properties at sp and sd metal single-crystal electrodes. In *Modern Aspects of Electrochemistry*, Plenum: New York, 1985; Vol. 16, pp 1-101.
4. Shi, Z.; Lipkowski, J.; Gamboa, M.; Zelenay, P.; Wieckowski, A., Investigations of SO_4^{2-} adsorption at the Au(111) electrode by chronocoulometry and radiochemistry. *J. Electroanal. Chem.* **1994**, *366*, 317-326.
5. Savich, W.; Sun, S. G.; Lipkowski, J.; Wieckowski, A., Determination of the sum of Gibbs excesses of sulfate and bisulfate adsorbed at the Pt(111) electrode surface using chronocoulometry and thermodynamics of the perfectly polarized electrode. *J. Electroanal. Chem.* **1995**, *388*, 233-237.
6. Garcia-Araez, N.; Climent, V.; Herrero, E.; Feliu, J.; Lipkowski, J., Thermodynamic studies of bromide adsorption at the Pt(111) electrode surface perchloric acid solutions: Comparison with other anions. *J. Electroanal. Chem.* **2006**, *591*, 149-158.
7. Climent, V.; Garcia-Araez, N.; Herrero, E.; Feliu, J., Potential of zero total charge of platinum single crystals: A local approach to stepped surfaces vicinal to Pt(111). *Russ. J. Electrochem.* **2006**, *42*, 1145-1160.
8. Garcia-Araez, N.; Climent, V.; Rodríguez, P.; Feliu, J. M., Thermodynamic analysis of (bi)sulphate adsorption on a Pt(111) electrode as a function of pH. *Electrochim. Acta* **2008**, *53*, 6793-6806.
9. Kuzume, A.; Herrero, E.; Feliu, J. M., Oxygen reduction on stepped platinum surfaces in acidic media. *J. Electroanal. Chem.* **2007**, *599*, 333-343.
10. Markovic, N. M.; Gasteiger, H. A.; Grgur, B. N.; Ross, P. N., Oxygen reduction reaction on Pt(111): effects of bromide. *J. Electroanal. Chem.* **1999**, *467*, 157-163.
11. Clavilier, J.; Orts, J. M.; Gómez, R.; Feliu, J. M.; Aldaz, A., On the nature of the charged species displaced by CO adsorption from platinum oriented electrodes in sulphuric acid solution. In *The Electrochemical Society Proceedings*, Conway, B. E.; Jerkiewicz, G., Eds. The Electrochemical Society, INC.: Pennington, NJ, 1994; Vol. 94-21, pp 167-183.
12. Feliu, J. M.; Orts, J. M.; Gómez, R.; Aldaz, A.; Clavilier, J., New information on the unusual adsorption states of Pt(111) in sulphuric acid solutions from potentiostatic adsorbate replacement by CO *J. Electroanal. Chem.* **1994**, *372*, 265-268.
13. Orts, J. M.; Gómez, R.; Feliu, J. M.; Aldaz, A.; Clavilier, J., Potentiostatic charge displacement by exchanging adsorbed species on Pt(111) electrodes—acidic electrolytes with specific anion adsorption *Electrochim. Acta* **1994**, *39*, 1519-1524.
14. Gómez, R.; Feliu, J. M.; Aldaz, A.; Weaver, M. J., Validity of double-layer charge-corrected voltammetry for assaying carbon monoxide coverages on ordered transition metals: comparisons with adlayer structures in electrochemical and ultrahigh vacuum environments. *Surf. Sci.* **1998**, *410*, 48-61.
15. Climent, V.; Gómez, R.; Feliu, J. M., Effect of increasing amount of steps on the potential of zero total charge of Pt(111) electrodes. *Electrochim. Acta* **1999**, *45*, 629-637.

16. Climent, V.; Coles, B. A.; Compton, R. G., Laser induced current transients applied to a Au(111) single crystal electrode. A general method for the measurement of potentials of zero charge of solid electrodes. *J. Phys. Chem. B* **2001**, *105*, 10669-10673.
17. Garcia-Araez, N.; Climent, V.; Herrero, E.; Feliu, J.; Lipkowski, J., Thermodynamic studies of chloride adsorption at the Pt(111) electrode surface from 0.1 M $HClO_4$ Solution. *J. Electroanal. Chem.* **2005**, *576*, 33-41.
18. Garcia-Araez, N.; Climent, V.; Rodriguez, P.; Feliu, J. M., Thermodynamic evidence for K^+-SO_4^{2-} ion pair formation on Pt(111). New insight into cation specific adsorption. *Phys. Chem. Chem. Phys.* **2010**, *12*, 12146-12152.
19. Garcia-Araez, N.; Climent, V.; Rodriguez, P.; Feliu, J. M., Elucidation of the chemical nature of adsorbed species for Pt(111) in H_2SO_4 solutions by thermodynamic analysis. *Langmuir* **2010**, *26*, 12408-12417.
20. Su, Z. F.; Climent, V.; Leitch, J.; Zamlynny, V.; Feliu, J. M.; Lipkowski, J., Quantitative SNIFTIRS studies of (bi)sulfate adsorption at the Pt(111) electrode surface. *Phys. Chem. Chem. Phys.* **2010**, *12*, 15231-15239.
21. Berna, A.; Delgado, J. M.; Orts, J. M.; Rodes, A.; Feliu, J. M., In-situ infrared study of the adsorption and oxidation of oxalic acid at single-crystal and thin-film gold electrodes: A combined external reflection infrared and ATR-SEIRAS approach. *Langmuir* **2006**, *22*, 7192-7202.
22. Delgado, J. M.; Berna, A.; Orts, J. M.; Rodes, A.; Feliu, J. M., In situ infrared study of the adsorption and surface acid-base properties of the anions of dicarboxylic acids at gold single crystal and thin-film electrodes. *J. Phys. Chem. C* **2007**, *111*, 9943-9952.
23. Rodes, A.; Pastor, E.; Iwasita, T., Structural efects on CO_2 reduction at Pt single-crystal electrodes: Part 2. Pt(111) and vicinal surfaces in the [0 -1 1] zone. *J. Electroanal. Chem.* **1994**, *373*, 167-175.
24. Iwasita, T.; Rodes, A.; Pastor, E., Vibrational spectroscopy of carbonate adsorbed on Pt(111) and Pt(110) single-crystal electrodes. *J. Electroanal. Chem.* **1995**, *383*, 181-189.
25. Berna, A.; Rodes, A.; Feliu, J. M.; Illas, F.; Gil, A.; Clotet, A.; Ricart, J. M., Structural and spectroelectrochemical study of carbonate and bicarbonate adsorbed on Pt(111) and Pd/Pt(111) electrodes. *J. Phys. Chem. B* **2004**, *108*, 17928-17939.
26. Berna, A.; Rodes, A.; Feliu, J. M., In-situ FTIR studies on the acid-base equilibria of adsorbed species on well-defined metal electrode surfaces. In *In-situ Spectroscopic Studies of Adsorption at the Electrode and Electrocatalysis*, Sun, S.-G.; Christensen, P. A.; Wieckowski, A., Eds. Elsevier: Amsterdam, 2007; pp 1-32.
27. Berna, A.; Climent, V.; Feliu, J. M., New understanding of the nature of OH adsorption on Pt(111) electrodes. *Electrochem. Commun.* **2007**, *9*, 2789-2794.
28. Korzeniewski, C.; Climent, V.; Feliu, J., Electrochemistry at platinum single crystal electrodes. In *Electroanalytical Chemistry: A Series of Advances*, Bard, A. J.; Zoski, C. G., Eds. CRC Press: Boca Raton, 2011; Vol. 24, pp 75-170.
29. Zamlynny, V.; Lipkowski, J., Quantitative SNIFTIR and PM IRAS of organic molecules at electrode surfaces. In *Advances in Electrochemical Science and Engineering*, Alkire, R. C.; Kolb, D. M.; Lipkowski, J., Eds. Wiley-VCH Verlag GmbH & Co.: Winheim, 2006; Vol. 9, pp 315-376.
30. Clavilier, J.; El Achi, K.; Rodes, A., In situ characterization of the Pt(S)-[n(111) x (111)] electrode surfaces using electrosorbed hydrogen for probing terrace an step sites. *J. Electroanal. Chem.* **1989**, *272*, 253-261.
31. Clavilier, J.; El Achi, K.; Rodes, A., Insitu probing of step and terrace sites on Pt(S)-n(111)x(111) electrodes. *Chem. Phys.* **1990**, *141*, 1-14.
32. Rodes, A.; El Achi, K.; Zamakhchari, M. A.; Clavilier, J., Hydrogen probing of step and terrace sites on Pt(S) [n(111) x (100)]. *J. Electroanal. Chem.* **1990**, *284*, 245-253.
33. Climent, V.; Feliu, J. M., Thirty years of platinum single crystal electrochemistry. *J. Solid State Electrochem.* **2011**, *15*, 1297-1315.

34. Weaver, M. J., Potentials of zero charge for platinum(111)-aqueous interfaces: A combined assessment from in-situ and ultrahigh-vacuum measurements. *Langmuir* **1998**, *14*, 3932-3936.
35. Cuesta, A., Measurement of the surface charge density of CO-saturated Pt(111) electrodes as a function of potential: The potential of zero charge of Pt(111). *Surf. Sci.* **2004**, *572*, 11-22.
36. Martinez-Hincapie, R.; Sebastian-Pascual, P.; Climent, V.; Feliu, J. M., Exploring the interfacial neutral pH region of Pt(111) electrodes. *Electrochem. Commun.* **2015**, *58*, 62-64.
37. Rizo, R.; Sitta, E.; Herrero, E.; Climent, V.; Feliu, J. M., Towards the understanding of the interfacial pH scale at Pt(111) electrodes. *Electrochim. Acta* **2015**, *162*, 138-145.
38. Griffiths, P. R.; De Haseth, J. A., *Fourier transform infrared spectrometry*, 2nd ed.; Wiley-Interscience: Hoboken, N.J., 2007, p xvii, 529 p.
39. Iwasita, T.; Nart, F. C., In-situ infrared Fourier Transform spectroscopy. A tool to characterize the electrode-electrolyte interface at a molecular level. VCH: Weinheim, 1995; pp 123-216.
40. Li, N.; Zamlynny, V.; Lipkowski, J.; Henglein, F.; Pettinger, B., In situ IR reflectance absorption spectroscopy studies of pyridine adsorption at the Au(110) electrode surface. *J. Electroanal. Chem.* **2002**, *524-525*, 43-53.
41. Osawa, M., Dynamic processes in electrochemical reactions studied by Surface-Enhanced Infrared Absorption Spectroscopy (SEIRAS). *Bull. Chem. Soc. Jpn.* **1997**, *70*, 2861-2880.
42. Wandlowski, T.; Ataka, K.; Pronkin, S.; Diesing, D., Surface enhanced infrared spectroscopy--Au(1 1 1-20nm)/sulphuric acid--new aspects and challenges. *Electrochim. Acta* **2004**, *49*, 1233-1247.
43. Falk, M.; Miller, A. G., Infrared-spectrum of carbon-dioxide in aqueous-solution. *Vib. Spectrosc.* **1992**, *4*, 105-108.
44. Lewis, G. N., *Valence and the structure of atoms and molecules*; Dover Publications: New York,, 1966, p 172 p.
45. Wien, M., About the validity of Ohm's laws for electrolytes in very high field forces. *Physikalische Zeitschrift* **1922**, *23*, 399-403.
46. Wien, M., On the validity of Ohm's laws for electrolytes in very high field forces. *Annalen Der Physik* **1924**, *73*, 161-181.
47. Wien, M., On a discrepancy from Ohm's law on electrolytes. *Annalen Der Physik* **1927**, *83*, 0327-0361.
48. Wien, M., Conductivity's tension effect in strong and weak acids. *Physikalische Zeitschrift* **1931**, *32*, 545-547.
49. Onsager, L., Deviations from Ohm's law in weak electrolytes. *J. Chem. Phys.* **1934**, *2*.
50. Gostisam, B.; Vielstich, W., Determination of rate constants of some weak acids with aid of rotating electrodes - Influence of electric-field in double-layer region. *Ber Bunsen Phys Chem* **1973**, *77*, 476-483.
51. Lasia, A., Modeling of hydrogen upd isotherms. *J. Electroanal. Chem.* **2004**, *562*, 23-31.
52. Climent, V.; Gómez, R.; Orts, J. M.; Feliu, J. M., Thermodynamic analysis of the temperature dependence of OH adsorption on Pt(111) and Pt(100) electrodes in acidic media in the absence of specific anion adsorption. *J. Phys. Chem. B* **2006**, *110*, 11344-11351.
53. Herrero, E.; Mostany, J.; Feliu, J. M.; Lipkowski, J., Thermodynamic studies of anion adsorption at the Pt(111) electrode surface in sulfuric acid solutions. *J. Electroanal. Chem.* **2002**, *534*, 79-89.
54. Bard, A. J.; Faulkner, L. R., *Electrochemical Methods. Fundamental and Applications*, 2nd ed.; John Wiley & Sons, Inc.: New York, 2001.
55. Buch, V.; Milet, A.; Vacha, R.; Jungwirth, P.; Devlin, J. P., Water surface is acidic. *Proc. Natl. Acad. Sci. U. S. A.* **2007**, *104*, 7342-7347.

	pH 1.43		pH 3.10	
	RHE	SHE	RHE	SHE
pztc/V	0.37	0.29	0.46	0.28
pzfc/V	0.35	0.27	0.46	0.28

Table 1. Values of the pztc and pzfc, measured versus RHE and SHE reference electrodes, for two different pH values, as indicated. Pztc are obtained from the integration of the voltammogram and CO displacement data. Pzfc are obtained from the extrapolation of the free charge in the double layer region considering a constant value of double layer capacity.

E/V SHE	$\sigma/\mu Ccm^{-2}$	Φ_2/V	surface pH
0.10	-12.2	-0.098	1.5
0.20	-5.3	-0.059	2.1
0.30	1.2	0.017	3.4
0.40	8.2	0.079	4.4

Table 2: values of the electric potential at the OHP, Φ_2, and surface pH values, at various potentials, calculated by Gouy Chapman Stern model, from the corresponding values of the free surface charge. The latter were extrapolated from the total charge curve corresponding to the CO_2 saturated solution with pH=3.1 (figure 1B).

Graphic TOC